Realization and Performance Evaluation of Join Process in User-Centric Cell-Free Networks

Yevhenii Shudrenko, Anna Maria Dewi Prajitno, Koojana Kuladinithi, Andreas Timm-Giel
Institute of Communication Networks
Hamburg University of Technology,
Hamburg, Germany
{yevhenii.shudrenko, anna.prajitno, koojana.kuladinithi, timm-giel}@tuhh.de

***Abstract*—Cell-free Massive MIMO has been proposed as an alternative to conventional cellular networks, where geographically distributed Access Points (APs) jointly serve multiple users through Dynamic Cooperation Clustering (DCC) to improve coverage and spectral efficiency. The first step in DCC is the join process, where UEs must find and synchronize to a master AP. This study proposes a message-level model of the UE-side and AP-side join procedures and evaluates it under contention-based CSMA/CA medium access. The proposed message-level model employs a three-way handshake consisting of a beacon, join request, and join response, with master AP selection based on the shortest distance. Results from OMNeT++ simulations under varying UE densities show that the proposed scheme allows UEs to successfully join the cell-free network. The join latency is primarily determined by the number of master AP changes, while the join success rate is dependent on AP capacity and spatial distribution of UEs. The proposed framework provides a practical realization of the join process and establishes a foundation for studying subsequent DCC procedures, particularly pilot assignment and cluster formation, in user-centric cell-free networks.**

***Index Terms*—Cell-free massive MIMO, dynamic cooperation clustering, user-centric networking, join process, AP selection, network simulation**

I. Introduction

For decades, cellular networks have served as the dominant infrastructure for wireless communications. However, the continuous growth in the number of connected devices has led to increasing demands for higher data rates, lower latency, and ubiquitous coverage.

Cell-free technology has emerged as a promising alternative to overcome the limitations of conventional cellular networks, particularly for users located at cell edges, where weak signal strength, reduced data rates, and increased latency are commonly experienced. The fundamental concept of cell-free networks is to eliminate cell boundaries: instead of being associated with a single base station, User Equipments (UEs) are jointly served by a large number of geographically distributed Access Points (APs) [1], [2]. This distributed architecture enables AP cooperation without fixed cell boundaries, thereby improving spectral efficiency, mitigating the disadvantages experienced by cell-edge users, and providing a more uniform quality of service throughout the coverage area [3]–[7].

In cell-free Massive Multiple Input Multiple Output (MIMO), the network infrastructure typically consists of a larger number of geographically distributed APs than active UEs within the coverage area. Nevertheless, this does not imply that every AP simultaneously serves every UE. In user-centric cell-free networks, each UE is served by a selected subset of APs, making it necessary to limit the the number of serving APs per UE [1], [2], [5], [8]. In practice, an AP may serve more UEs than the number of antennas it possesses, reflecting the user-centric nature of the architecture. To enable efficient cooperation, APs are organized into clusters through user-centric Dynamic Cooperation Clustering (DCC), where a subset of APs dynamically cooperates to serve each UE [2], [9].

To form clusters in DCC, candidate APs require channel information for the users they may serve. In Time-Division Duplex (TDD)-based cell-free systems, this information is obtained through uplink pilot transmission, where UEs transmit pilot signals that allow APs to estimate the wireless channel. Based on the obtained Channel State Information (CSI), the available information allows each AP to independently determine whether to participate in serving a particular UE within the cooperation cluster [2], [8].

TDD is commonly used when channel reciprocity is required. In TDD systems, uplink pilot signals are used to estimate the downlink channel due to channel reciprocity. However, the number of orthogonal pilot sequences is limited by the channel coherence time, requiring pilot sequences to be reused among different UEs. This reuse leads to pilot contamination, where an AP cannot accurately distinguish the channel estimates of different UEs sharing the same pilot sequence [2], [9].

The DCC clustering process consists of three main steps, beginning with the selection of a master AP by the UE based on information obtained during the join process. Once selected, the master AP assigns a pilot sequence to the UE, enabling pilot transmission. Through this transmission, nearby APs obtain CSI estimates and determine whether to participate in serving the UE [2], [8].

Although previous studies have considered the master AP selection procedure in user-centric cell-free networks, the join

This research was supported by the project 'Next Generation City Networking' (Grant No. 19DZ24004) at the Hanseatic Wireless Innovation Competence Center (HAWICC). The project is funded by the Federal Ministry of Transport via the German Center for Future Mobility (DZM).

process is typically represented at an abstract level without explicitly modeling the underlying signaling mechanisms. As a result, the impact of practical aspects, including message exchanges, packet losses, and AP capacity constraints, on the join process remains insufficiently understood. This work addresses this gap through message-level simulations of the master AP appointment procedure and evaluates its performance under different network conditions. The performance is evaluated in terms of join latency, join success rate, UE-to-master-AP distance, the number of candidate master AP changes, and the loss rate of join request/response under different network densities and AP capacity configurations using contention-based MAC layer.

II. Related work

Several studies have investigated AP selection and AP–UE association as strategies for determining the serving AP subset in cell-free and user-centric networks [10]–[12]. For instance, Freitas et al. [10] follow a different AP-selection approach from the DCC-based procedure described in [2]. Their method does not require the UE to appoint a master AP as a prior step for forming a cooperative AP cluster. Instead, the UE first connects to an intermediate AP subset through matched decisions between the UE and APs, which is then expanded into a final AP cluster. Meanwhile, Dao and Kim [11] and Vu et al. [12] primarily focus on determining or optimizing the serving AP set. Specifically, Dao and Kim [11] select APs based on effective channel gain, whereas Vu et al. [12] jointly consider AP selection and power allocation. However, these works do not model the DCC-based master AP appointment and join procedure.

In [8] Björnson and Sanguinetti propose a scalable cell-free massive MIMO framework based on DCC for initial access, pilot assignment, and cluster formation. In their approach, each UE selects the AP with the strongest large-scale fading coefficient as its master AP, assuming that the UE reaches this AP through a standard random access procedure. However, the join process itself is treated abstractly, and the underlying message exchanges and protocol interactions are not explicitly modeled. Consequently, the impact of practical factors, such as message losses, AP capacity limitations, and signaling delays, on the master AP selection process remains unexplored. And while [13] proposes improved algorithms for initial access and pilot assignment and evaluates their performance under user mobility using ray-traced channel models, the MAC layer is largely abstracted away. Consequently, its impact on the UE–AP message exchange, including protocol timing, beacon transmission intervals, packet collisions, and retransmissions, is not captured. To address this gap, this work implements and evaluates the message-level join procedure associated with the master AP appointment stage described in [2], [8], enabling the investigation of its performance under realistic network constraints.

Table I: Simulation configuration

Parameter	Value
Link layer	IEEE 802.15.4 CSMA/CA
Radio center frequency	2.45 GHz
Channel bandwidth	2.8 MHz
Transmit power	0.3 mW
Receiver sensitivity	−100 dBm
Modulation	DSSS − OQPSK − 16
Path loss module	BreakpointPathLoss
Beacon size	73 B
Join request, response size	65 B
Number of APs	112
Number of UEs	$2, 25, 50, \ldots, 575$
Communication range	≈ 80 m
Simulation duration	1000 s
Number of repetitions	10
Confidence level	95%
AP discovery window	20 s

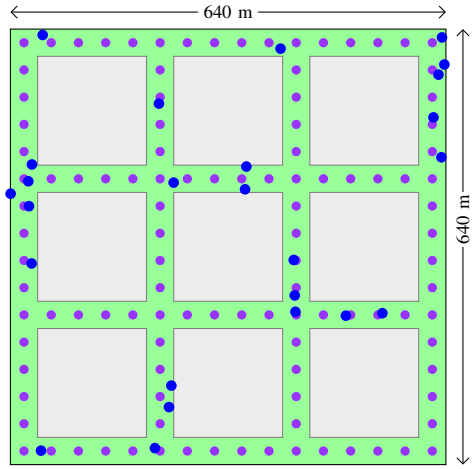


Figure 1: Simulated street-layout area with predefined AP positions indicated by purple circles and UEs distributed uniformly at random, indicated by blue circles.

III. Design/Methodologies/Implementation

This section presents the network topology, simulation setup, and the proposed join process algorithm used to evaluate master AP selection under AP capacity constraints.

A. Network and Simulation Setup

The network simulation is implemented in OMNeT++ with INET framework, using the configuration listed in Table I. In Fig. 1 the layout of the simulated cell-free network is shown, where the green area represents deployable streets of 40 m width and the grey blocks represent building blocks where UEs cannot be deployed, each measuring $160\,\mathrm{m} \times 160\,\mathrm{m}$. APs are predefined, centered within the street zones, spaced 40 m apart, while UEs are uniformly randomly distributed across the street area. All nodes remain stationary throughout the simulation.

This configuration enables observation of the join process as UE density increases while AP deployment remains fixed. To better reflect realistic network conditions, the simulation also incorporates basic elements of the later DCC steps involving

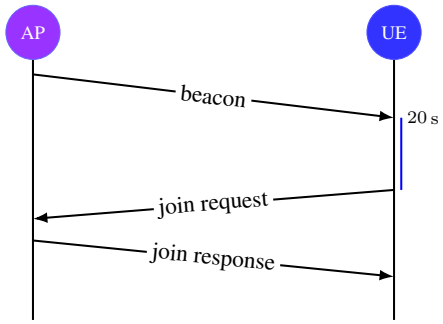


Figure 2: Three-way handshake mechanism for master AP selection with AP discovery window of 20 s.

pilot assignment [2], [8], where the master AP broadcasts a message to nearby APs after sending a positive join response in order to notify them of the pilot assigned to newly joined UE. Thus, for the channel access we used already available IEEE 802.15.4 CSMA/CA with beacon transmissions over a shared channel. It is used to simulate a busier traffic condition, as the network is expected to experience higher traffic once the full DCC steps are implemented.

B. Join Process Algorithm

In this work, the communication procedure is based on a three-way handshake mechanism as illustrated in Fig. 2. APs broadcast beacons with their location coordinates with intervals following the Trickle algorithm [14] to avoid congestion. Upon reception, a UE stores the AP ID (MAC address) and its coordinates in the candidate master AP (MAP) list, from which the nearest AP is selected first.

First, the UE collects beacons from nearby APs to identify the best master AP. The discovery phase employs a sliding window, which starts upon reception of the first beacon and is restarted whenever a beacon from a previously undiscovered AP is received. The discovery window duration was chosen empirically and set to 20 s in this study. Given the minimum Trickle timer interval of $I_{\min} = 2^3 = 8\,\text{ms}$, a UE can receive approximately 12 beacons from each nearby AP within this window. Meanwhile, duplicate beacons from already discovered APs are ignored, ensuring that the UE has sufficient time to discover all APs within its communication range before transmitting a join request.

Then, a join request is transmitted by a UE to the first candidate master AP. A join response can be positive or negative: a positive one indicating that the UE has successfully joined the network and selected its master AP, categorized as a join success, while a negative join response indicates a rejection from the currently selected candidate master AP because that AP has reached its capacity limit.

To handle join requests, an AP maintains a pending-UE and an accepted-UE list, each of size C_{AP}. The pending-UE list temporarily stores the UE ID (MAC address) upon receiving a join request, and removes it either when a MAC-layer packet loss signal for the join response is received, or when the UE ID is moved to the accepted-UE list. The accepted-UE list

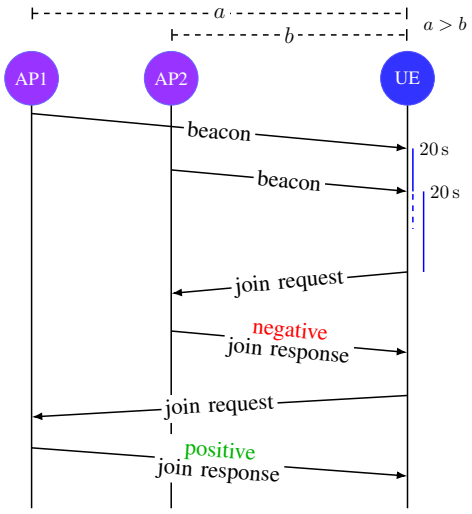


Figure 3: Example of UE changing master AP due to negative join response.

stores the IDs of UEs that have successfully acknowledged the positive join response on the link-layer and joined the AP.

Based on the state of these lists, the join response type is determined. If the accepted-UE list has reached the AP capacity, the AP sends a negative join response. If the UE ID is already listed in the pending-UE list, the AP retransmits a positive join response. If the pending-UE list is full, the AP ignores the join request, allowing the UE to retransmit the join request according to the link-layer retransmission mechanism. If the maximum retransmission threshold is reached, the UE selects a new candidate master AP. If both lists have available capacity, the UE ID is added to the pending-UE list and the AP sends a positive join response.

Upon receiving a negative join response, the UE removes the current master AP candidate from the candidate list and selects the next closest candidate. The UE then resumes the join procedure from the second step by transmitting a join request to the newly selected AP, as illustrated in Fig. 3.

If the candidate-MAP list becomes empty, all candidate APs have been requested and all have returned negative join responses, resulting in a join failure. Consequently, the join procedure has two possible outcomes: join success and join failure. The AP-side and UE-side workflows of the proposed join procedure are illustrated in Fig. 4 and Fig. 5, respectively.

IV. Analysis of Results

This section evaluates the behavior of the proposed join process under varying UE densities and AP capacity C_{AP} constraints, based on the Key Performance Indicators (KPIs) such as join latency, join success rate, distance to master AP, number of master AP changes, as well as join request/response loss rate. Commonly used notation is summarized in Table II.

Join latency is the time difference between the first beacon signal and the positive join response received by UE:

$$T_{\text{join}} = t_{\text{pj}} - t_{\text{fb}}, \tag{1}$$

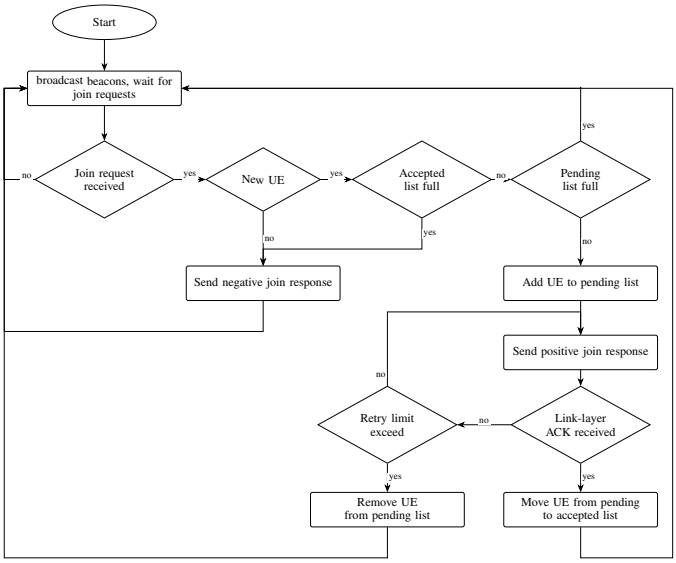


Figure 4: AP during the join process.

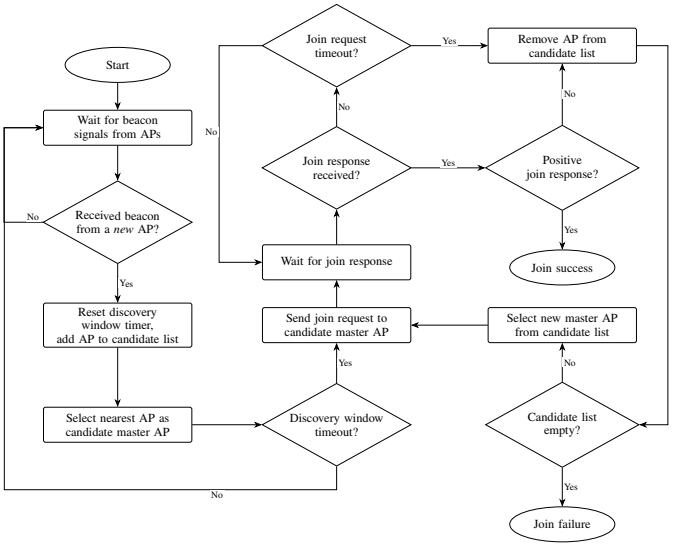


Figure 5: UE during the join process.

where t_{pj} is the timestamp of a positive join response, t_{fb} is the timestamp of the first beacon signal, as shown in Fig. 6. The join success rate is the ratio of the number of UEs receiving a positive join response (N_{joined}) to the total number of UEs (N_{UE}) in the network. The distance to master AP in simulation

Table II: Notation glossary

Variable	Meaning
C_{AP}	AP capacity
C_{tot}	Aggregate capacity of all APs
$N_{\mathrm{AP}}, N_{\mathrm{UE}}$	Number of APs, UEs
N_{joined}	Number of UEs that got assigned a master AP
T_{join}	Join latency
R	MAC-layer retransmission threshold
ρ_{AP}	AP utilization

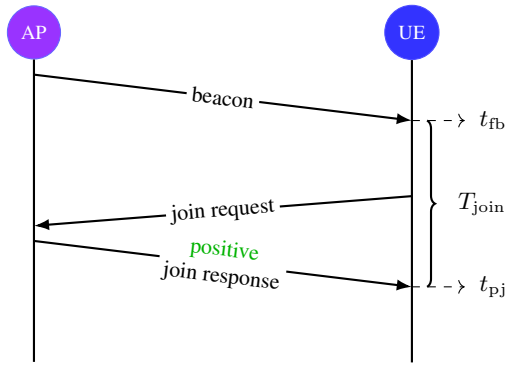


Figure 6: Successful join process with the timing parameters to define join latency calculation.

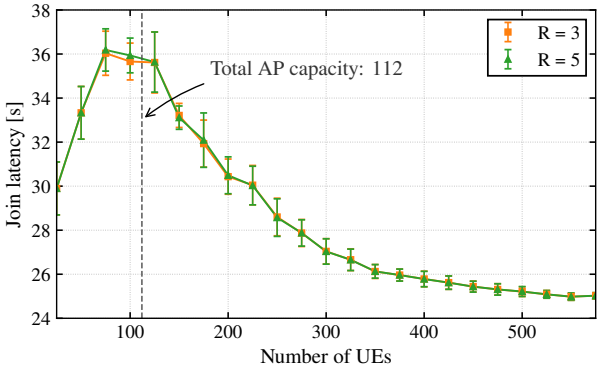


Figure 7: Join latency with $C_{\mathrm{AP}} = 1$ and variable R.

is computed using the location information that APs put into their beacons. The number of master AP changes reflects how often a UE received a negative join response and had to request the next AP from its candidate list.

Let N_{AP} denote the total number of APs in the network and C_{AP} be the maximum number of UEs that each AP can serve (AP capacity), which may be limited, e.g., by its processing capabilities or the size of antenna array. Since the total AP capacity C_{tot} is defined as

$$C_{\mathrm{tot}} = N_{\mathrm{AP}} C_{\mathrm{AP}}, \tag{2}$$

the average AP utilization ρ_{AP} is then

$$\rho_{\mathrm{AP}} = \frac{N_{\mathrm{joined}}}{C_{\mathrm{tot}}}. \tag{3}$$

A. Results and Analysis

First, the join latency and join success rate are evaluated under variable MAC-layer retransmission threshold R. Based on Fig. 7 and Fig. 8, R has no impact on both KPIs, implying that packet collisions are infrequent and are not the reason some UEs fail to join the network. The latter can be attributed to the uniform spatial distribution of UEs with respect to fixed AP placement. Therefore, the recommended value of $R = 3$ from IEEE 802.15.4 is used for all subsequent simulations.

The join success rate drops with increasing number of UEs due to the limited AP capacity. A higher UE density means

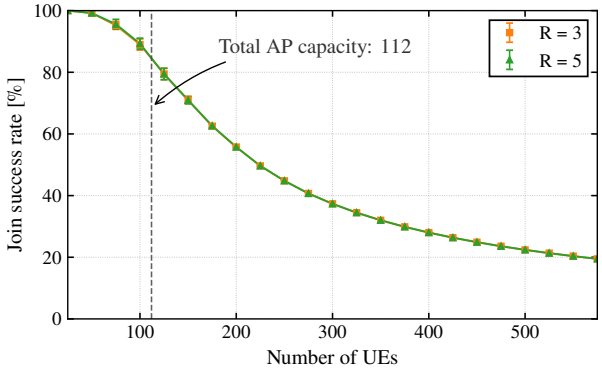


Figure 8: Join success rate with $C_{\mathrm{AP}} = 1$ and variable R.

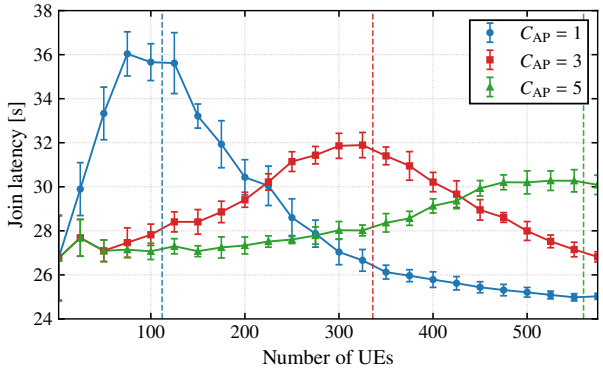


Figure 9: Join latency of successfully joined UEs for different C_{AP} values.

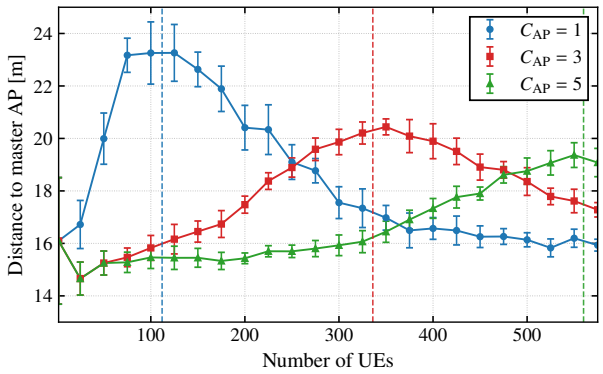


Figure 10: Average distance to master AP for different C_{AP} values, vertical dashed lines are C_{tot}.

increased probability that multiple UEs compete for the *same* AP, causing more UEs to receive a negative join response and be forced to try selecting a new master AP. Even before the number of users reaches the theoretical aggregated capacity limit of $C_{\mathrm{tot}} = C_{\mathrm{AP}} N_{\mathrm{AP}} = 112$, there are users not able to join the network due to the sparse placement of APs. The uniform random distribution of users results in small clusters, see Fig. 1, which cannot be fully served by the neighboring APs if C_{AP} is too low.

The join latency initially increases with the number of users, reaching its peak around C_{tot}. As contention grows, multiple UEs compete for the same preferred master AP. Once that AP reaches its capacity, affected UEs must repeat the join procedure with their next-best candidate AP, increasing the overall latency.

Beyond C_{tot}, the join latency decreases because the number of master AP changes drops. At such high user densities, most APs are occupied immediately after their first beacon broadcast. Consequently, UEs whose initial attempt fails typically find no capacity available at alternative candidate APs, eliminating additional join request cycles and reducing the average latency.

With R fixed, the evaluation focuses on the impact of C_{AP} on the join process. Fig. 9 shows join latency trend similar to Fig. 7 across all C_{AP} values with the peaks shifted with increasing C_{tot}. The peak join latency slightly decreases with higher C_{AP} due to fewer master AP changes, as recorded in Fig. 11. Higher C_{AP} allows more users to join their preferred master AP and avoid extra join request-response cycles.

Fig. 12 shows that, due to the uniform spatial distribution of users and the sparse, even AP placement, not all users are able to join the network even when $N_{\mathrm{UE}} < C_{\mathrm{tot}}$. Some users are simply outside the communication range of APs with remaining capacity. However, with increasing C_{AP} the success rate at exactly C_{tot} is also increasing, implying that higher AP capacity still alleviates user clustering. This is further supported by Fig. 13, which shows that even when $N_{\mathrm{UE}} > C_{\mathrm{tot}}$, $\rho_{\mathrm{AP}} < 100\%$, i.e., some APs retain available capacity but remain unreachable to the unserved UEs.

Lastly, the loss rate of join requests and join responses is visualized in Fig. 14. The primary source of losses are packet collisions due to contention-based CSMA/CA. Join requests exhibit slightly higher loss rate than join responses due to the fact UEs that are in the vicinity of the same AP receive its beacon and have synchronized discovery windows, resulting in simultaneous transmission of join requests. Since UEs have no real-time information on the occupancy status of each AP, they continue transmitting join requests to candidate APs from their list, increasing MAC-layer contention. The loss of join responses is mostly due to the hidden node problem, given an even AP spacing as well as AP broadcasts after each successful join response. Despite these loss rates, AP utilization continues to increase with UE density, see Fig. 13, indicating that $R = 3$ results in sufficiently reliable join process.

V. Conclusion

This work bridges the gap between theoretical DCC formulations and their protocol-level realization by explicitly describing the signaling procedure required for the master AP selection. A three-way handshake mechanism is implemented, enabling the evaluation of join performance under varying AP capacity constraints and UE densities with contention-based medium access.

The results show that the join latency is primarily determined by the number of join request and join response cycles,

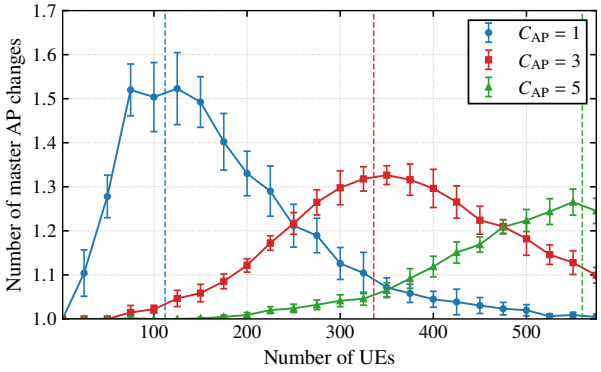


Figure 11: Average number of master AP changes for different C_{AP} values, vertical dashed lines are C_{tot}.

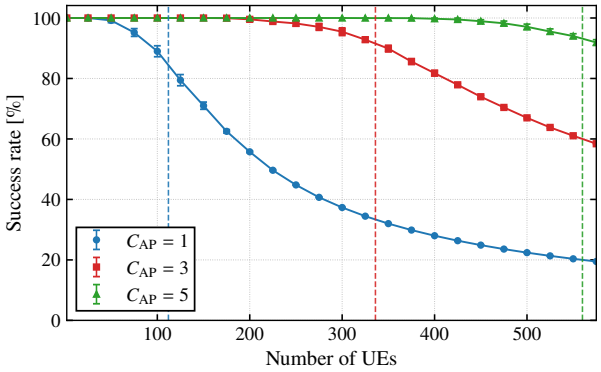


Figure 12: Join success rate for different C_{AP} values.

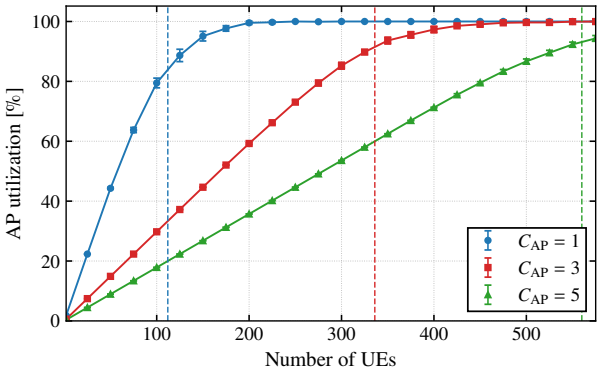


Figure 13: Average ρ_{AP} for different C_{AP} values.

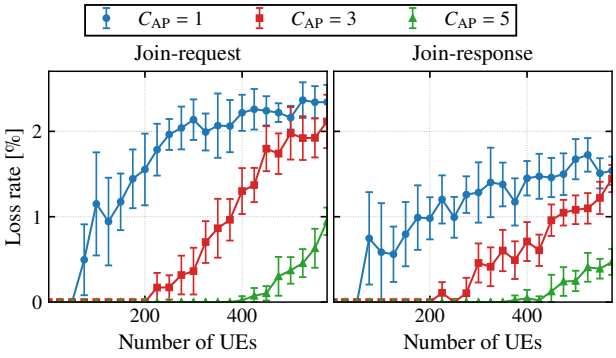


Figure 14: Join request and join response loss rates for different C_{AP}.

which corresponds to the number of candidate master AP changes. The loss rates of join request and join response messages below 3 % in the highest UE density scenario hint that a contention-based MAC like CSMA/CA is a feasible option for the join process in cell-free networks.

This feasibility study demonstrates the practical realization of the join procedure in DCC and provides insights into the impact of network parameters on its performance. The proposed framework is sufficiently flexible to be extended to other master AP selection strategies, including CSI-based AP selection. It provides a foundation for a complete DCC implementation and the evaluation of pilot assignment strategies. Future work will consider UE mobility and realistic physical layer, which directly impact the join process performance.

References

[1] S. Buzzi and C. D'Andrea, "Cell-free massive mimo: User-centric approach," *IEEE Wireless Communications Letters*, vol. 6, no. 6, pp. 706–709, Dec. 2017.

[2] Ö. T. Demir, E. Björnson, and L. Sanguinetti, "Foundations of user-centric cell-free massive MIMO," *Foundations and Trends® in Signal Processing*, vol. 14, no. 3–4, pp. 162–472, 2021.

[3] H. A. Ammar, R. Adve, S. Shahbazpanahi, G. Boudreau, and K. V. Srinivas, "User-centric cell-free massive mimo networks: A survey of opportunities, challenges and solutions," *IEEE Communications Surveys & Tutorials*, vol. 24, no. 1, pp. 611–652, 2022.

[4] H. Q. Ngo, A. Ashikhmin, H. Yang, E. G. Larsson, and T. L. Marzetta, "Cell-free massive mimo versus small cells," *IEEE Transactions on Wireless Communications*, vol. 16, no. 3, pp. 1834–1850, Mar. 2017.

[5] E. Björnson and L. Sanguinetti, "Making cell-free massive mimo competitive with mmse processing and centralized implementation," *IEEE Transactions on Wireless Communications*, vol. 19, no. 1, pp. 77–90, Jan. 2020.

[6] P. Liu, K. Luo, D. Chen, and T. Jiang, "Spectral efficiency analysis of cell-free massive mimo systems with zero-forcing detector," *IEEE Transactions on Wireless Communications*, vol. 19, no. 2, pp. 795–807, Feb. 2020.

[7] A. Papazafeiropoulos, P. Kourtessis, M. D. Renzo, S. Chatzinotas, and J. M. Senior, "Performance analysis of cell-free massive mimo systems: A stochastic geometry approach," *IEEE Transactions on Vehicular Technology*, vol. 69, no. 4, pp. 3523–3537, Apr. 2020.

[8] E. Björnson and L. Sanguinetti, "Scalable cell-free massive MIMO systems," *IEEE Transactions on Communications*, vol. 68, no. 7, pp. 4247–4261, Jul. 2020.

[9] S. Chen, J. Zhang, J. Zhang, E. Björnson, and B. Ai, "A survey on user-centric cell-free massive mimo systems," *Digital Communications and Networks*, vol. 8, no. 5, pp. 695–719, 2022.

[10] M. Freitas, D. Souza, G. Borges, *et al.*, "Matched-decision AP selection for user-centric cell-free massive MIMO networks," *IEEE Transactions on Vehicular Technology*, vol. 72, no. 5, pp. 6375–6391, May 2023.

[11] H. T. Dao and S. Kim, "Effective channel gain-based access point selection in cell-free massive MIMO systems," *IEEE Access*, vol. 8, pp. 108 127–108 132, 2020.

[12] T. X. Vu, S. Chatzinotas, S. ShahbazPanahi, and B. Ottersten, "Joint power allocation and access point selection for cell-free massive MIMO," in *IEEE International Conference on Communications (ICC)*, 2020, pp. 1–6.

[13] M. Zaher, E. Björnson, and M. Petrova, "Soft handover procedures in mmwave cell-free massive mimo networks," *IEEE Transactions on Wireless Communications*, vol. 23, no. 6, pp. 6124–6138, 2024.

[14] P. Levis, T. H. Clausen, O. Gnawali, J. Hui, and J. Ko, *The Trickle Algorithm*, RFC 6206, Mar. 2011.